

Improved Measurements of Branching Fractions and CP Asymmetries in $B \rightarrow \eta h$ Decays

K. Abe,⁹ K. Abe,⁴⁷ I. Adachi,⁹ H. Aihara,⁴⁹ K. Aoki,²³ K. Arinstein,² Y. Asano,⁵⁴
 T. Aso,⁵³ V. Aulchenko,² T. Aushev,¹³ T. Aziz,⁴⁵ S. Bahinipati,⁵ A. M. Bakich,⁴⁴
 V. Balagura,¹³ Y. Ban,³⁶ S. Banerjee,⁴⁵ E. Barberio,²² M. Barbero,⁸ A. Bay,¹⁹ I. Bedny,²
 U. Bitenc,¹⁴ I. Bizjak,¹⁴ S. Blyth,²⁵ A. Bondar,² A. Bozek,²⁹ M. Bračko,^{9,21,14}
 J. Brodzicka,²⁹ T. E. Browder,⁸ M.-C. Chang,⁴⁸ P. Chang,²⁸ Y. Chao,²⁸ A. Chen,²⁵
 K.-F. Chen,²⁸ W. T. Chen,²⁵ B. G. Cheon,⁴ C.-C. Chiang,²⁸ R. Chistov,¹³ S.-K. Choi,⁷
 Y. Choi,⁴³ Y. K. Choi,⁴³ A. Chuvikov,³⁷ S. Cole,⁴⁴ J. Dalseno,²² M. Danilov,¹³ M. Dash,⁵⁶
 L. Y. Dong,¹¹ R. Dowd,²² J. Dragic,⁹ A. Drutskoy,⁵ S. Eidelman,² Y. Enari,²³ D. Epifanov,²
 F. Fang,⁸ S. Fratina,¹⁴ H. Fujii,⁹ N. Gabyshev,² A. Garmash,³⁷ T. Gershon,⁹ A. Go,²⁵
 G. Gokhroo,⁴⁵ P. Goldenzweig,⁵ B. Golob,^{20,14} A. Gorišek,¹⁴ M. Grosse Perdekamp,³⁸
 H. Guler,⁸ R. Guo,²⁶ J. Haba,⁹ K. Hara,⁹ T. Hara,³⁴ Y. Hasegawa,⁴² N. C. Hastings,⁴⁹
 K. Hasuko,³⁸ K. Hayasaka,²³ H. Hayashii,²⁴ M. Hazumi,⁹ T. Higuchi,⁹ L. Hinz,¹⁹ T. Hojo,³⁴
 T. Hokuue,²³ Y. Hoshi,⁴⁷ K. Hoshina,⁵² S. Hou,²⁵ W.-S. Hou,²⁸ Y. B. Hsiung,²⁸
 Y. Igarashi,⁹ T. Iijima,²³ K. Ikado,²³ A. Imoto,²⁴ K. Inami,²³ A. Ishikawa,⁹ H. Ishino,⁵⁰
 K. Itoh,⁴⁹ R. Itoh,⁹ M. Iwasaki,⁴⁹ Y. Iwasaki,⁹ C. Jacoby,¹⁹ C.-M. Jen,²⁸ R. Kagan,¹³
 H. Kakuno,⁴⁹ J. H. Kang,⁵⁷ J. S. Kang,¹⁶ P. Kapusta,²⁹ S. U. Kataoka,²⁴ N. Katayama,⁹
 H. Kawai,³ N. Kawamura,¹ T. Kawasaki,³¹ S. Kazi,⁵ N. Kent,⁸ H. R. Khan,⁵⁰
 A. Kibayashi,⁵⁰ H. Kichimi,⁹ H. J. Kim,¹⁸ H. O. Kim,⁴³ J. H. Kim,⁴³ S. K. Kim,⁴¹
 S. M. Kim,⁴³ T. H. Kim,⁵⁷ K. Kinoshita,⁵ N. Kishimoto,²³ S. Korpar,^{21,14} Y. Kozakai,²³
 P. Krizan,^{20,14} P. Krokovny,⁹ T. Kubota,²³ R. Kulasiri,⁵ C. C. Kuo,²⁵ H. Kurashiro,⁵⁰
 E. Kurihara,³ A. Kusaka,⁴⁹ A. Kuzmin,² Y.-J. Kwon,⁵⁷ J. S. Lange,⁶ G. Leder,¹²
 S. E. Lee,⁴¹ Y.-J. Lee,²⁸ T. Lesiak,²⁹ J. Li,⁴⁰ A. Limosani,⁹ S.-W. Lin,²⁸ D. Liventsev,¹³
 J. MacNaughton,¹² G. Majumder,⁴⁵ F. Mandl,¹² D. Marlow,³⁷ H. Matsumoto,³¹
 T. Matsumoto,⁵¹ A. Matyja,²⁹ Y. Mikami,⁴⁸ W. Mitaroff,¹² K. Miyabayashi,²⁴ H. Miyake,³⁴
 H. Miyata,³¹ Y. Miyazaki,²³ R. Mizuk,¹³ D. Mohapatra,⁵⁶ G. R. Moloney,²² T. Mori,⁵⁰
 A. Murakami,³⁹ T. Nagamine,⁴⁸ Y. Nagasaka,¹⁰ T. Nakagawa,⁵¹ I. Nakamura,⁹
 E. Nakano,³³ M. Nakao,⁹ H. Nakazawa,⁹ Z. Natkaniec,²⁹ K. Neichi,⁴⁷ S. Nishida,⁹
 O. Nitoh,⁵² S. Noguchi,²⁴ T. Nozaki,⁹ A. Ogawa,³⁸ S. Ogawa,⁴⁶ T. Ohshima,²³ T. Okabe,²³
 S. Okuno,¹⁵ S. L. Olsen,⁸ Y. Onuki,³¹ W. Ostrowicz,²⁹ H. Ozaki,⁹ P. Pakhlov,¹³ H. Palka,²⁹
 C. W. Park,⁴³ H. Park,¹⁸ K. S. Park,⁴³ N. Parslow,⁴⁴ L. S. Peak,⁴⁴ M. Pernicka,¹²
 R. Pestotnik,¹⁴ M. Peters,⁸ L. E. Piilonen,⁵⁶ A. Poluektov,² F. J. Ronga,⁹ N. Root,²
 M. Rozanska,²⁹ H. Sahoo,⁸ M. Saigo,⁴⁸ S. Saitoh,⁹ Y. Sakai,⁹ H. Sakamoto,¹⁷
 H. Sakaue,³³ T. R. Sarangi,⁹ M. Satapathy,⁵⁵ N. Sato,²³ N. Satoyama,⁴² T. Schietinger,¹⁹
 O. Schneider,¹⁹ P. Schönmeier,⁴⁸ J. Schümann,²⁸ C. Schwanda,¹² A. J. Schwartz,⁵
 T. Seki,⁵¹ K. Senyo,²³ R. Seuster,⁸ M. E. Sevier,²² T. Shibata,³¹ H. Shibuya,⁴⁶
 J.-G. Shiu,²⁸ B. Shwartz,² V. Sidorov,² J. B. Singh,³⁵ A. Somov,⁵ N. Soni,³⁵ R. Stamen,⁹
 S. Stanič,³² M. Starič,¹⁴ A. Sugiyama,³⁹ K. Sumisawa,⁹ T. Sumiyoshi,⁵¹ S. Suzuki,³⁹
 S. Y. Suzuki,⁹ O. Tajima,⁹ N. Takada,⁴² F. Takasaki,⁹ K. Tamai,⁹ N. Tamura,³¹
 K. Tanabe,⁴⁹ M. Tanaka,⁹ G. N. Taylor,²² Y. Teramoto,³³ X. C. Tian,³⁶ K. Trabelsi,⁸

Y. F. Tse,²² T. Tsuboyama,⁹ T. Tsukamoto,⁹ K. Uchida,⁸ Y. Uchida,⁹ S. Uehara,⁹
T. Uglov,¹³ K. Ueno,²⁸ Y. Unno,⁹ S. Uno,⁹ P. Urquijo,²² Y. Ushiroda,⁹ G. Varner,⁸
K. E. Varvell,⁴⁴ S. Villa,¹⁹ C. C. Wang,²⁸ C. H. Wang,²⁷ M.-Z. Wang,²⁸ M. Watanabe,³¹
Y. Watanabe,⁵⁰ L. Widhalm,¹² C.-H. Wu,²⁸ Q. L. Xie,¹¹ B. D. Yabsley,⁵⁶ A. Yamaguchi,⁴⁸
H. Yamamoto,⁴⁸ S. Yamamoto,⁵¹ Y. Yamashita,³⁰ M. Yamauchi,⁹ Heyoung Yang,⁴¹
J. Ying,³⁶ S. Yoshino,²³ Y. Yuan,¹¹ Y. Yusa,⁴⁸ H. Yuta,¹ S. L. Zang,¹¹ C. C. Zhang,¹¹
J. Zhang,⁹ L. M. Zhang,⁴⁰ Z. P. Zhang,⁴⁰ V. Zhilich,² T. Ziegler,³⁷ and D. Zürcher¹⁹

(The Belle Collaboration)

¹*Aomori University, Aomori*

²*Budker Institute of Nuclear Physics, Novosibirsk*

³*Chiba University, Chiba*

⁴*Chonnam National University, Kwangju*

⁵*University of Cincinnati, Cincinnati, Ohio 45221*

⁶*University of Frankfurt, Frankfurt*

⁷*Gyeongsang National University, Chinju*

⁸*University of Hawaii, Honolulu, Hawaii 96822*

⁹*High Energy Accelerator Research Organization (KEK), Tsukuba*

¹⁰*Hiroshima Institute of Technology, Hiroshima*

¹¹*Institute of High Energy Physics,*

Chinese Academy of Sciences, Beijing

¹²*Institute of High Energy Physics, Vienna*

¹³*Institute for Theoretical and Experimental Physics, Moscow*

¹⁴*J. Stefan Institute, Ljubljana*

¹⁵*Kanagawa University, Yokohama*

¹⁶*Korea University, Seoul*

¹⁷*Kyoto University, Kyoto*

¹⁸*Kyungpook National University, Taegu*

¹⁹*Swiss Federal Institute of Technology of Lausanne, EPFL, Lausanne*

²⁰*University of Ljubljana, Ljubljana*

²¹*University of Maribor, Maribor*

²²*University of Melbourne, Victoria*

²³*Nagoya University, Nagoya*

²⁴*Nara Women's University, Nara*

²⁵*National Central University, Chung-li*

²⁶*National Kaohsiung Normal University, Kaohsiung*

²⁷*National United University, Miao Li*

²⁸*Department of Physics, National Taiwan University, Taipei*

²⁹*H. Niewodniczanski Institute of Nuclear Physics, Krakow*

³⁰*Nippon Dental University, Niigata*

³¹*Niigata University, Niigata*

³²*Nova Gorica Polytechnic, Nova Gorica*

³³*Osaka City University, Osaka*

³⁴*Osaka University, Osaka*

³⁵*Panjab University, Chandigarh*

³⁶*Peking University, Beijing*

³⁷*Princeton University, Princeton, New Jersey 08544*

³⁸*RIKEN BNL Research Center, Upton, New York 11973*

³⁹*Saga University, Saga*

⁴⁰*University of Science and Technology of China, Hefei*

⁴¹*Seoul National University, Seoul*

⁴²*Shinshu University, Nagano*

⁴³*Sungkyunkwan University, Suwon*

⁴⁴*University of Sydney, Sydney NSW*

⁴⁵*Tata Institute of Fundamental Research, Bombay*

⁴⁶*Toho University, Funabashi*

⁴⁷*Tohoku Gakuin University, Tagajo*

⁴⁸*Tohoku University, Sendai*

⁴⁹*Department of Physics, University of Tokyo, Tokyo*

⁵⁰*Tokyo Institute of Technology, Tokyo*

⁵¹*Tokyo Metropolitan University, Tokyo*

⁵²*Tokyo University of Agriculture and Technology, Tokyo*

⁵³*Toyama National College of Maritime Technology, Toyama*

⁵⁴*University of Tsukuba, Tsukuba*

⁵⁵*Utkal University, Bhubaneswer*

⁵⁶*Virginia Polytechnic Institute and State University, Blacksburg, Virginia 24061*

⁵⁷*Yonsei University, Seoul*

Abstract

We report improved measurements of B decays with an η meson in the final state using 357 fb^{-1} of data collected by the Belle detector at the KEKB e^+e^- collider. We observe the decays $B^\pm \rightarrow \eta\pi^\pm$ and $B^\pm \rightarrow \eta K^\pm$; the measured branching fractions are $\mathcal{B}(B^\pm \rightarrow \eta\pi^\pm) = (3.9 \pm 0.5(\text{stat}) \pm 0.2(\text{sys})) \times 10^{-6}$ and $\mathcal{B}(B^\pm \rightarrow \eta K^\pm) = (2.2 \pm 0.4(\text{stat}) \pm 0.1(\text{sys})) \times 10^{-6}$. Their corresponding CP -violating asymmetries are measured to be $-0.10 \pm 0.11(\text{stat}) \pm 0.02(\text{sys})$ for $\eta\pi^\pm$ and $-0.55 \pm 0.19(\text{stat})_{-0.03}^{+0.04}(\text{sys})$ for ηK^\pm . No significant signal is found for $B^0 \rightarrow \eta K^0$ decays; the upper limit on the branching fraction at the 90% confidence level is $\mathcal{B}(B^0 \rightarrow \eta K^0) < 1.9 \times 10^{-6}$.

PACS numbers: 13.25.Hw, 12.15.Hh, 11.30.Er

Charmless B decays provide a rich sample to understand B decay dynamics and to search for CP violation. It has been suggested [1] that direct CP violation could be large in $B^+ \rightarrow \eta\pi^+$ [2] and $B^+ \rightarrow \eta K^+$ decays due to penguin-tree interference. In our earlier measurements [3], no CP -violating asymmetry (A_{CP}) was seen for the $\eta\pi^+$ mode. Belle's central value of A_{CP} for ηK^+ was large in magnitude and negative, but statistics were limited even for the branching fraction measurement. In the most recent update from the BaBar collaboration [4], the previous negative A_{CP} values with $\sim 2\sigma$ significance for both ηK^+ and $\eta\pi^+$ modes have moved to within $\sim 1\sigma$ deviation from zero. Because experimental uncertainties on CP asymmetries and branching fractions are still large, it is necessary to analyze larger data sample.

In this paper, we report improved measurements of branching fractions and partial rate asymmetries for $B \rightarrow \eta h$ decays, where h is a K or π meson. The partial rate asymmetry for charged B decays is defined to be:

$$A_{CP} = \frac{N(B^- \rightarrow \eta h^-) - N(B^+ \rightarrow \eta h^+)}{N(B^- \rightarrow \eta h^-) + N(B^+ \rightarrow \eta h^+)}, \quad (1)$$

where $N(B^-)$ is the yield for the $B^- \rightarrow \eta h^-$ decay and $N(B^+)$ denotes that of the charge conjugate mode. The data sample consists of 386 million $B\bar{B}$ pairs (357 fb^{-1}) collected with the Belle detector at the KEKB e^+e^- asymmetric-energy (3.5 on 8 GeV) collider [6] operating at the $\Upsilon(4S)$ resonance.

The Belle detector is a large-solid-angle magnetic spectrometer that consists of a silicon vertex detector (SVD), a 50-layer central drift chamber (CDC), an array of aerogel threshold Čerenkov counters (ACC), a barrel-like arrangement of time-of-flight scintillation counters (TOF), and an electromagnetic calorimeter (ECL) comprised of CsI(Tl) crystals located inside a superconducting solenoid coil that provides a 1.5 T magnetic field. An iron flux-return located outside of the coil is instrumented to detect K_L^0 mesons and to identify muons (KLM). The detector is described in detail elsewhere [7]. In August 2003, the three-layer SVD was replaced by a four-layer radiation tolerant device. The data sample used in this analysis consists of 140 fb^{-1} of data with the old SVD (Set I) and 217 fb^{-1} with the new one (Set II).

The event selection and candidate reconstruction are similar to that documented in our previous paper [3]. Here, we only give a brief description of event selection. Two η decay channels are considered in this analysis: $\eta \rightarrow \gamma\gamma$ ($\eta_{\gamma\gamma}$) and $\eta \rightarrow \pi^+\pi^-\pi^0$ ($\eta_{3\pi}$). We require photons from η and π^0 candidates to have laboratory energies above 50 MeV. In the $\eta_{\gamma\gamma}$ reconstruction, the energy asymmetry, defined as the absolute value of the energy difference in the laboratory frame between the two photons divided by their energy sum, must be less than 0.9. Neither photon is allowed to pair with any other photon with at least 100 MeV energy to form a π^0 candidate. Candidate π^0 mesons are selected by requiring the two-photon invariant mass to be in the mass window between $115 \text{ MeV}/c^2$ and $152 \text{ MeV}/c^2$. The momentum vector of each photon is then readjusted to constrain the mass of the photon pair to the nominal π^0 mass.

Candidate $\eta_{3\pi}$ mesons are reconstructed by combining a π^0 with at least 250 MeV/ c laboratory momentum with a pair of oppositely charged tracks that originate from the interaction point (IP). We make the following requirements on the invariant mass of the η candidates in both data sets: $516 \text{ MeV}/c^2 < M_{\gamma\gamma} < 569 \text{ MeV}/c^2$ for $\eta_{\gamma\gamma}$ and $539 \text{ MeV}/c^2 < M_{3\pi} < 556 \text{ MeV}/c^2$ for $\eta_{3\pi}$. After the selection of each candidate, the η mass constraint is implemented by readjusting the momentum vectors of the daughter particles.

Charged tracks are required to come from the IP. Charged kaons and pions, which are combined with η mesons to form B candidates, are identified using a $K(\pi)$ likelihood $L_K(L_\pi)$ obtained by combining information from the CDC (dE/dx), the TOF and the ACC. Discrimination between kaons and pions is achieved through a requirement on the likelihood ratio $L_K/(L_\pi + L_K)$. Charged tracks with likelihood ratios greater than 0.6 are regarded as kaons, and less than 0.4 as pions. Furthermore, charged tracks that are positively identified as electrons or muons are rejected. The K/π identification efficiencies and misidentification rates are determined from a sample of $D^{*+} \rightarrow D^0\pi^+$, $D^0 \rightarrow K^-\pi^+$ decays. In reference [8] we reported that in both data sets π^+ has a higher efficiency than π^- while the kaon identification efficiency is higher for K^- than K^+ . The efficiency difference introduces a bias in A_{CP} which needs to be corrected. K_S^0 candidates are reconstructed from pairs of oppositely-charged tracks with an invariant mass ($M_{\pi\pi}$) between 480 and 516 MeV/ c^2 . Each candidate must have a displaced vertex with a flight direction consistent with that of a K_S^0 originating from the IP.

Candidate B mesons are identified using the beam constrained mass, $M_{bc} = \sqrt{E_{\text{beam}}^2 - P_B^2}$, and the energy difference, $\Delta E = E_B - E_{\text{beam}}$, where E_{beam} is the run-dependent beam energy in the $\Upsilon(4S)$ rest frame and is determined from $B \rightarrow D^{(*)}\pi$ events, and P_B and E_B are the momentum and energy of the B candidate in the $\Upsilon(4S)$ rest frame. The resolutions on M_{bc} and ΔE are about 3 MeV/ c^2 and 20–30 MeV, respectively. Events with $M_{bc} > 5.2$ GeV/ c^2 and $|\Delta E| < 0.3$ GeV are selected for the analysis.

The dominant background comes from the $e^+e^- \rightarrow q\bar{q}$ continuum, where $q = u, d, s$ or c . To distinguish signal from the jet-like continuum background, event shape variables and B flavor tagging information are employed. We combine information of correlated shape variables into a Fisher discriminant [9] and compute the likelihood as a product of probabilities of this discriminant and $\cos\theta_B$, where θ_B is the angle between the B flight direction and the beam direction in the $\Upsilon(4S)$ rest frame. A likelihood ratio, $\mathcal{R} = \mathcal{L}_s/(\mathcal{L}_s + \mathcal{L}_{q\bar{q}})$, is formed from signal (\mathcal{L}_s) and background ($\mathcal{L}_{q\bar{q}}$) likelihoods, obtained using events from the signal Monte Carlo (MC) and from data with $M_{bc} < 5.26$ GeV/ c^2 , respectively. Additional background discrimination is provided by B flavor tagging. An event that contains a lepton (high quality tagging) is more likely to be a $B\bar{B}$ event so a looser \mathcal{R} requirement can be applied. We divide the data into six sub-samples based on the quality of flavor tagging [10] (see details in [3]). Continuum suppression is achieved by applying a mode dependent requirement on \mathcal{R} for events in each sub-sample in Set I and Set II according to $N_s^{\text{exp}}/\sqrt{N_s^{\text{exp}} + N_{q\bar{q}}^{\text{exp}}}$, where N_s^{exp} is the expected signal from MC and $N_{q\bar{q}}^{\text{exp}}$ denotes the number of background events estimated from data.

From MC all other backgrounds are found to be negligible except for the $\eta K^+ \leftrightarrow \eta\pi^+$ reflection, due to $K^+ \leftrightarrow \pi^+$ misidentification, and the feed-down from charmless B decays, predominantly $B \rightarrow \eta K^*(892)$ and $B \rightarrow \eta\rho(770)$. We include these two components in the fit used to extract the signal.

The signal yields and partial rate asymmetries are obtained using an extended unbinned maximum-likelihood (ML) fit with input variables M_{bc} and ΔE . The likelihood is defined as:

$$\mathcal{L} = \exp^{-\sum_j N_j} \times \prod_i (\sum_j N_j \mathcal{P}_j) \quad \text{and} \quad (2)$$

$$\mathcal{P}_j = \frac{1}{2} [1 - q_i \cdot \mathcal{A}_{CPj}] P_j(M_{bc_i}, \Delta E_i), \quad (3)$$

where i is the identifier of the i -th event, $P(M_{bc}, \Delta E)$ is the two-dimensional probability density function (PDF) in M_{bc} and ΔE , q indicates the B meson flavor, $B^+(q = +1)$ or $B^-(q = -1)$, N_j is the number of events for the category j , which corresponds to either signal, $q\bar{q}$ continuum, a reflection due to K - π misidentification, or background from other charmless B decays. For the neutral B mode, \mathcal{P}_j in the equation above is simply $P_j(M_{bci}, \Delta E_i)$ and there is no reflection component.

Since the efficiency of particle identification is slightly different for positively and negatively charged particles, the raw asymmetry defined in Eq. 1 must be corrected. This efficiency difference results in an A_{CP} bias of -0.005 (0.005) for $\eta\pi$ (ηK). The bias is subtracted from the value obtained for the raw asymmetry.

The signal peak positions and resolutions in M_{bc} and ΔE are adjusted according to the data-MC differences using large control samples of $B \rightarrow D\pi$ and $\bar{D}^0 \rightarrow K^+\pi^-\pi^0/\pi^0\pi^0$ decays. The continuum background in ΔE is described by a first or second order polynomial while the M_{bc} distribution is parameterized by an ARGUS function, $f(x) = x\sqrt{1-x^2} \exp[-\xi(1-x^2)]$, where x is M_{bc} divided by half of the total center of mass energy [11]. Thus the continuum PDF is the product of an ARGUS function and a polynomial, where ξ and the coefficients of the polynomial are free parameters. The PDFs of the reflection and charmless B backgrounds are modelled as two-dimensional smooth functions, obtained using large MC samples.

All the signal and background yields and their partial rate asymmetries are free parameters in the fit except for the reflection components, where the A_{CP} and the normalizations are fixed to expectations based on the $B^+ \rightarrow \eta K^+$ and $B^+ \rightarrow \eta\pi^+$ partial rate asymmetries and branching fractions, as well as $K^+ \leftrightarrow \pi^+$ fake rates. The reflection yield and A_{CP} are first input with the assumed values and are then recalculated according to our measured results.

Table I shows the measured branching fractions for each decay mode as well as other quantities associated with the measurements. The efficiency for each mode is determined using MC simulation and corrected for the discrepancy between data and MC using the control samples. Other than the particle identification performance discrepancy reported earlier [3], our MC slightly overestimates the detection efficiency of soft π^0 s in Set II, which results in a 4.3% correction for the $\eta_{3\pi}$ mode. The combined branching fraction of two data sets are computed as the sum of the yield divided by its efficiency in each set divided by the number of B mesons. The combined branching fraction of the two η decay modes is obtained from the weighted average assuming the errors are Gaussian. Systematic uncertainties in the fit due to the uncertainties in the signal PDFs are estimated by performing the fit after varying their peak positions and resolutions by one standard deviation. In $B^\pm \rightarrow \eta\pi^\pm$, the reflection yields in Set I (Set II) are estimated to be 3.4 (5.5) events for the $\eta_{\gamma\gamma}$ mode and 1.1 (2.0) for $\eta_{3\pi}$. And in $B^\pm \rightarrow \eta K^\pm$, the reflection yields are 3.2 (6.5) for $\eta_{\gamma\gamma}$ and 1.3 (2.2) for $\eta_{3\pi}$. The reflection yields and their A_{CP} values are varied by one standard deviation in the fit to obtain the corresponding systematic uncertainties. The quadratic sum of the deviations from the central value gives the systematic uncertainty in the fit, which ranges from 3% to 6%. For each systematic check, the statistical significance is taken as the square root of the difference between the value of $-2 \ln \mathcal{L}$ for zero signal yield and the best-fit value. We regard the smallest value as our significance including the systematic uncertainty. The number of B^+B^- and $B^0\bar{B}^0$ pairs are assumed to be equal.

The performance of the \mathcal{R} requirement is studied by checking the data-MC efficiency ratio using the $B^+ \rightarrow \bar{D}^0\pi^+$ control sample. The obtained systematic error is 2.0–3.3%.

TABLE I: Detection efficiency (ϵ) including sub-decay branching fraction, yield, significance (Sig.), measured branching fraction (\mathcal{B}), the 90% C.L. upper limit (UL) and A_{CP} for the $B \rightarrow \eta h$ decays. The first errors in columns 3, 5 and 7 are statistical and the second errors are systematic.

Mode	$\epsilon(\%)$	Yield	Sig.	$\mathcal{B}(10^{-6})$	UL(10^{-6})	A_{CP}
$B^\pm \rightarrow \eta\pi^\pm$			10.9	$3.9 \pm 0.5 \pm 0.2$		$-0.10 \pm 0.11 \pm 0.02$
$\eta_{\gamma\gamma}\pi^\pm$			8.7	$3.9_{-0.5}^{+0.6} \pm 0.2$		$0.08 \pm 0.14 \pm 0.02$
Set I	9.12	$71.5_{-12.5}^{+13.3} \pm 2.0$	7.0	$5.2_{-0.9}^{+1.0} \pm 0.3$		$0.14 \pm 0.18 \pm 0.02$
Set II	9.34	$68.3_{-14.9-2.9}^{+15.8+2.7}$	5.1	$3.1 \pm 0.7 \pm 0.2$		$0.00 \pm 0.22_{-0.03}^{+0.02}$
$\eta_{3\pi}\pi^\pm$			6.7	$3.8_{-0.8}^{+0.9} \pm 0.3$		$-0.54 \pm 0.22 \pm 0.02$
Set I	3.26	$16.1_{-5.7}^{+6.6} \pm 0.8$	3.3	$3.2_{-1.2}^{+1.3} \pm 0.3$		$-0.10 \pm 0.38_{-0.03}^{+0.02}$
Set II	3.53	$33.7_{5.8-2.2}^{+9.3+2.0}$	5.8	$4.1_{-1.0}^{+1.1} \pm 0.3$		$-0.76_{-0.27-0.04}^{+0.26+0.03}$
$B^\pm \rightarrow \eta K^\pm$			7.1	$2.2 \pm 0.4 \pm 0.1$		$-0.55 \pm 0.19_{-0.03}^{+0.04}$
$\eta_{\gamma\gamma}K^\pm$			5.8	$2.0 \pm 0.5_{-0.1}^{+0.2}$		$-0.71_{-0.27-0.04}^{+0.24+0.05}$
Set I	8.35	$27.0_{-9.0-2.3}^{+10.0+2.1}$	3.3	$2.1_{-0.7}^{+0.8} \pm 0.2$		$-0.44_{-0.37}^{+0.34} \pm 0.03$
Set II	8.47	$39.0_{-12.1-2.8}^{+13.0+2.7}$	4.5	$2.0_{-0.6}^{+0.7} \pm 0.2$		$-0.94_{-0.41}^{+0.32} \pm 0.07$
$\eta_{3\pi}K^\pm$			4.1	$2.3_{-0.6-0.1}^{+0.8+0.2}$		$-0.28_{-0.31-0.03}^{+0.29+0.04}$
Set I	3.03	$7.3_{-4.3-0.8}^{+5.4+1.0}$	2.2	$1.6_{-0.9}^{+1.2} \pm 0.2$		$-0.66_{-1.16-0.10}^{+0.67+0.13}$
Set II	3.19	$21.2_{-6.8-0.8}^{+7.7+0.9}$	3.5	$2.8_{-0.9}^{+1.0} \pm 0.2$		$-0.20_{-0.33}^{+0.34} \pm 0.03$
$B^0 \rightarrow \eta K^0$			2.1	$0.9 \pm 0.6 \pm 0.1$	< 1.9	
$\eta_{\gamma\gamma}K^0$			1.0	$0.6_{-0.6}^{+0.7} \pm 0.1$	< 2.2	
Set I	3.06	$-1.6_{-3.1-0.4}^{+4.3+0.5}$	–	$-0.3_{-0.7}^{+0.9} \pm 0.1$	< 1.7	
Set II	3.17	$9.0_{-6.3}^{+7.2} \pm 0.7$	1.4	$1.2_{-0.8}^{+1.0} \pm 0.1$	< 3.1	
$\eta_{3\pi}K^0$			1.8	$1.5_{-1.0}^{+1.2} \pm 0.1$	< 3.9	
Set I	0.90	$3.5_{-2.6-0.5}^{+3.5+0.3}$	1.5	$2.3_{-1.9}^{+2.5} \pm 0.3$	< 6.0	
Set II	1.00	$2.4_{-2.4-0.3}^{+3.4+0.2}$	1.0	$1.0_{-1.0}^{+1.5} \pm 0.1$	< 3.7	

The systematic errors on the charged track reconstruction are estimated to be around 1% per track using partially reconstructed D^* events. The π^0 and $\eta_{\gamma\gamma}$ reconstruction efficiency is verified by comparing the π^0 decay angular distribution with the MC prediction, and by measuring the ratio of the branching fractions for the two D decay channels: $\overline{D}^0 \rightarrow K^+\pi^-$ and $\overline{D}^0 \rightarrow K^+\pi^-\pi^0$. We assign a 3.5% (4.0 %) error for the π^0 and $\eta_{\gamma\gamma}$ reconstruction in Set I (Set II). The K_S^0 reconstruction is verified by comparing the ratio of $D^+ \rightarrow K_S^0\pi^+$ and $D^+ \rightarrow K^-\pi^+\pi^+$ yields. The resulting K_S^0 detection systematic errors for Set I and Set II are 4.4% and 4.0%, respectively. The uncertainty in the number of $B\overline{B}$ events is 1%. The final systematic error is obtained by first summing all correlated errors linearly and then quadratically summing the uncorrelated errors.

Figure 1 shows the M_{bc} and ΔE projections after requiring events to satisfy $-0.10 \text{ GeV} < \Delta E < 0.08 \text{ GeV}$ and $M_{bc} > 5.27 \text{ GeV}/c^2$, respectively. No significant signal is observed for the $B^0 \rightarrow \eta K^0$ meson mode. Significant signals are observed for charged B decays; the corresponding M_{bc} and ΔE projections for B^+ and B^- samples are shown in Figs. 2 and 3. The A_{CP} results for the two η decay modes in two data sets are combined assuming that the errors are Gaussian. No significant asymmetry is observed for the $\eta\pi^\pm$ mode while an

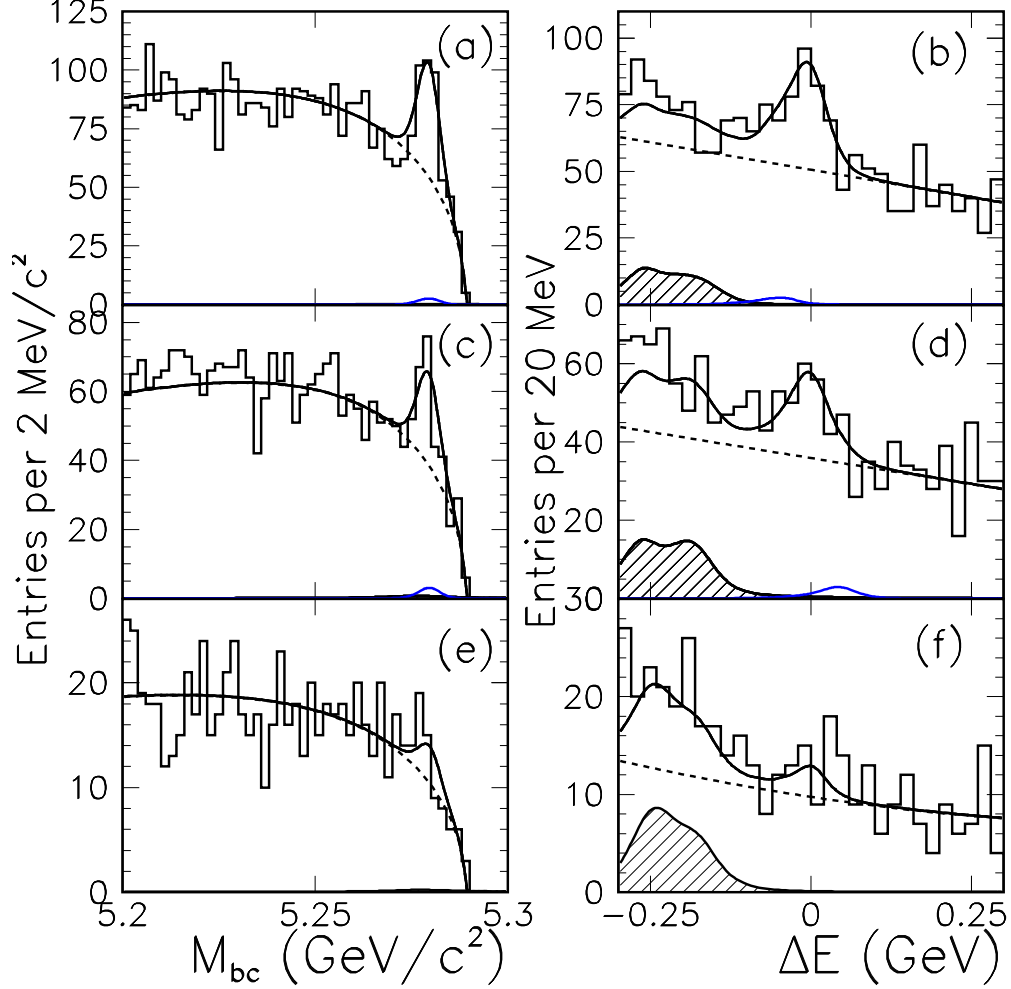


FIG. 1: M_{bc} and ΔE projections for (a,b) $B^\pm \rightarrow \eta\pi^\pm$, (c,d) $B^\pm \rightarrow \eta K^\pm$, and (e,f) $B^0 \rightarrow \eta K^0$ decays with the $\eta_{\gamma\gamma}$ and $\eta_{3\pi}$ modes combined. Open histograms are data, solid curves are the fit functions, dashed lines show the continuum contributions and shaded histograms are the feed-down component from charmless B decays. The small contributions around $M_{bc} = 5.28 \text{ GeV}/c^2$ and $\Delta E = \pm 0.05 \text{ GeV}$ in (a)-(d) are the reflection backgrounds from $B^\pm \rightarrow \eta K^\pm$ and $B^\pm \rightarrow \eta\pi^\pm$.

excess of B^+ over B^- decays is seen in the ηK^\pm mode, giving a large negative A_{CP} value.

In summary, we have observed $B^\pm \rightarrow \eta\pi^\pm$ and $B^\pm \rightarrow \eta K^\pm$ decays; their branching fractions are measured to be $(3.9 \pm 0.5 \pm 0.2) \times 10^{-6}$ and $(2.2 \pm 0.4 \pm 0.1) \times 10^{-6}$, respectively. The central values of our measurements in both modes are 1.4σ smaller than the results [4] reported by the BaBar collaboration. Our A_{CP} measurement for $B^\pm \rightarrow \eta\pi^\pm$, $-0.10 \pm 0.11 \pm 0.02$, is consistent with no asymmetry. However, the partial rate asymmetry for $B^\pm \rightarrow \eta K^\pm$ remains large in magnitude and negative, $A_{CP} = -0.55 \pm 0.19^{+0.04}_{-0.03}$, which is 2.9σ from zero. Larger data samples are needed to verify this large CP asymmetry. Finally, no significant $B^0 \rightarrow \eta K^0$ signal is found and we assign an upper limit at the 90% confidence level of $\mathcal{B}(B^0 \rightarrow \eta K^0) < 1.9 \times 10^{-6}$.

We thank the KEKB group for the excellent operation of the accelerator, the KEK Cryogenics group for the efficient operation of the solenoid, and the KEK computer group and the National Institute of Informatics for valuable computing and Super-SINET network

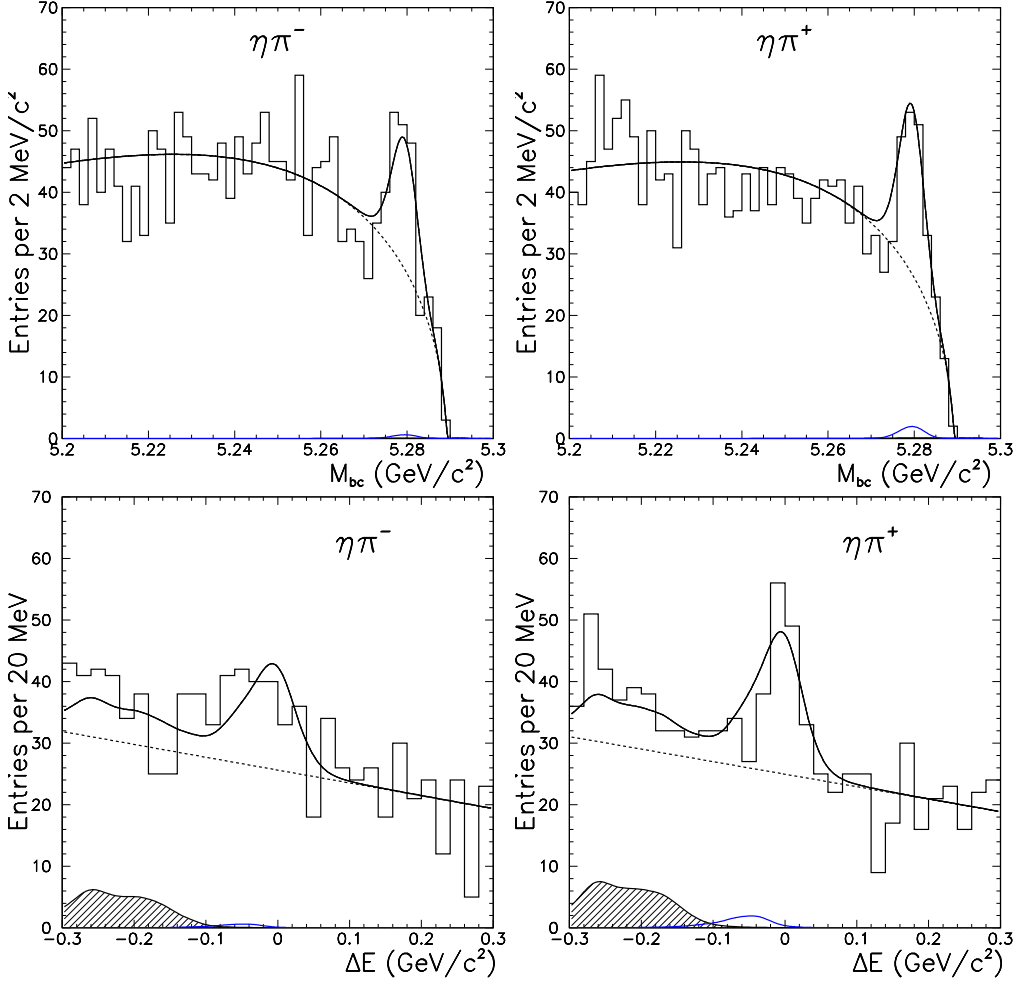


FIG. 2: M_{bc} and ΔE projections for (left) $B^- \rightarrow \eta\pi^-$ and (right) $B^+ \rightarrow \eta\pi^+$ with the $\eta_{\gamma\gamma}$ and $\eta_{3\pi}$ modes combined. Open histograms are data, solid curves are the fit functions, dashed lines show the continuum contributions and shaded histograms are the contributions from charmless B decays. The small contributions near $M_{bc} = 5.28 \text{ GeV}/c^2$ and $\Delta E = -0.05 \text{ GeV}$ are the backgrounds from misidentified $B^\pm \rightarrow \eta K^\pm$ (reflections).

support. We acknowledge support from the Ministry of Education, Culture, Sports, Science, and Technology of Japan and the Japan Society for the Promotion of Science; the Australian Research Council and the Australian Department of Education, Science and Training; the National Science Foundation of China under contract No. 10175071; the Department of Science and Technology of India; the BK21 program of the Ministry of Education of Korea and the CHEP SRC program of the Korea Science and Engineering Foundation; the Polish State Committee for Scientific Research under contract No. 2P03B 01324; the Ministry of Science and Technology of the Russian Federation; the Ministry of Education, Science and Sport of the Republic of Slovenia; the National Science Council and the Ministry of Education of Taiwan; and the U.S. Department of Energy.

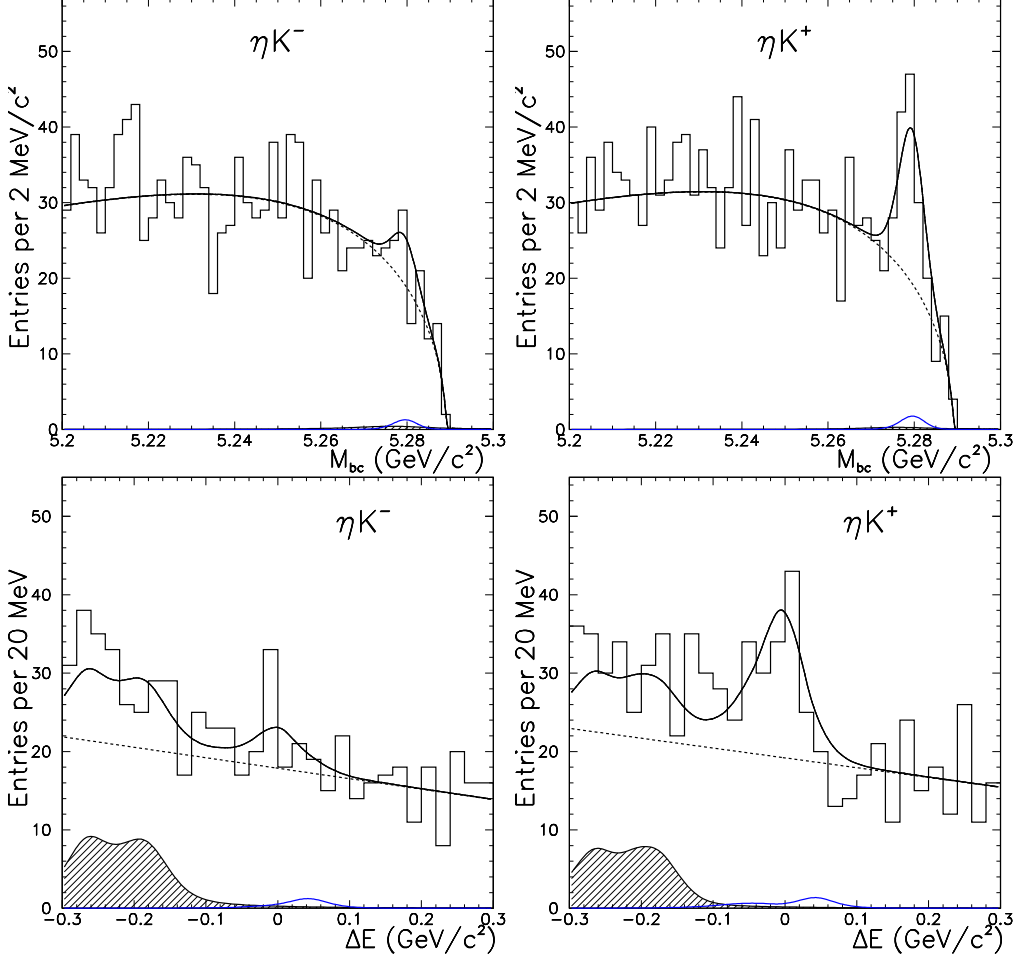


FIG. 3: M_{bc} and ΔE projections for (left) $B^- \rightarrow \eta K^-$ and (right) $B^+ \rightarrow \eta K^+$ with the $\eta_{\gamma\gamma}$ and $\eta_{3\pi}$ modes combined. Open histograms are data, solid curves are the fit functions, dashed lines show the continuum contributions and shaded histograms are the contributions from charmless B decays. The small contributions near $M_{bc} = 5.28 \text{ GeV}/c^2$ and $\Delta E = 0.05 \text{ GeV}/c^2$ are the backgrounds from misidentified $B^\pm \rightarrow \eta\pi^\pm$ (reflections).

-
- [1] M. Bander, D. Silverman, and A. Soni, Phys. Rev. Lett. **43**, 242 (1979); M.-Z. Yang and Y.-D. Yang, Nucl. Phys. B **609**, 409 (2001); M. Beneke and M. Neubert, Nucl. Phys. B **651**, 225 (2003); S. Barshay, D. Rein, and L.M. Sehgal, Phys. Lett. B **259**, 475 (1991); A. S. Dighe, M. Gronau, and J. L. Rosner, Phys. Rev. Lett. **79**, 4333 (1997).
- [2] Throughout this paper, the inclusion of the charge conjugate mode decay is implied unless otherwise stated.
- [3] Belle Collaboration, P. Chang *et al.*, Phys. Rev. D **71**, 091106(R) (2005).
- [4] BaBar Collaboration, B. Aubert *et al.*, hep-ex/0503035.
- [5] Y.-Y. Keum and A. I. Sanda, Phys. Rev. D **67**, 054009 (2003); C.-W. Chiang, M. Gronau, J.L. Rosner and D. A. Suprun, Phys. Rev. D **70**, 034020 (2004).
- [6] S. Kurokawa and E. Kikutani, Nucl. Instr. and Meth. A **499**, 1 (2003), and other papers

included in this volume.

- [7] Belle Collaboration, A. Abashian *et al.*, Nucl. Instr. and Meth. A **479**, 117 (2002).
- [8] Belle Collaboration, Y. Chao *et al.*, Phys. Rev. Lett. **93**, 191802 (2004).
- [9] R. A. Fisher, Ann. Eugenics **7**, 179 (1936).
- [10] Belle Collaboration, H. Kakuno *et al.*, Nucl. Instr. and Meth. A **533**, 516 (2004).
- [11] ARGUS Collaboration, H. Albrecht *et al.*, Phys. Lett. B **241**, 278 (1990).